Provided for non-commercial research and education use.
Not for reproduction, distribution or commercial use.

This article appeared in a journal published by Elsevier. The attached copy is furnished to the author for internal non-commercial research and education use, including for instruction at the authors institution and sharing with colleagues.

Other uses, including reproduction and distribution, or selling or licensing copies, or posting to personal, institutional or third party websites are prohibited.

In most cases authors are permitted to post their version of the article (e.g. in Word or Tex form) to their personal website or institutional repository. Authors requiring further information regarding Elsevier's archiving and manuscript policies are encouraged to visit:

http://www.elsevier.com/copyright

Author's personal copy

Journal of Luminescence 129 (2009) 148–152

Contents lists available at ScienceDirect

Journal of Luminescence

journal homepage: www.elsevier.com/locate/jlumin

Rapid thermal annealing effects on the structural and optical properties of ZnO films deposited on Si substrates

Yueh-Chien Lee [a,*], Sheng-Yao Hu [b], Walter Water [c], Kwong-Kau Tiong [d], Zhe-Chuan Feng [e], Yen-Ting Chen [e], Jen-Ching Huang [f], Jyh-Wei Lee [f], Chia-Chih Huang [a], Jyi-Lai Shen [a], Mou-Hong Cheng [a]

[a] Department of Electronic Engineering and Research Center for Micro/Nano Technology, Tungnan University, Taipei, Taiwan, ROC
[b] Department of Electrical Engineering, Tung Fang Institute of Technology, Hunei Township, Kaohsiung County, Taiwan, ROC
[c] Department of Electronic Engineering, National Formosa University, Yunlin, Taiwan, ROC
[d] Department of Electrical Engineering, National Taiwan Ocean University, Keelung, Taiwan, ROC
[e] Graduate Institute of Electro-Optical Engineering and Department of Electrical Engineering, National Taiwan University, Taipei, Taiwan, ROC
[f] Department of Mechanical Engineering and Research Center for Micro/Nano Technology, Tungnan University, Taipei, Taiwan, ROC

ARTICLE INFO

Article history:
Received 22 December 2007
Received in revised form
8 May 2008
Accepted 2 September 2008
Available online 20 September 2008

PACS:
42.70.−a
78.30.Fs
78.55.−m

Keywords:
Zinc oxide
Annealing
Photoluminescence
X-ray diffraction

ABSTRACT

The structural and optical properties of ZnO films deposited on Si substrate following rapid thermal annealing (RTA) have been investigated by X-ray diffraction (XRD), atomic force microscopy (AFM), and photoluminescence (PL) measurements. After RTA treatment, the XRD spectra have shown an effective relaxation of the residual compressive stress, an increase of the intensity and narrowing of the full-width at half-maximum (FWHM) of the (0 0 2) diffraction peak of the as-grown ZnO film. AFM images show roughening of the film surface due to increase of grain size after RTA. The PL spectrum reveals a significant improvement in the UV luminescence of ZnO films following RTA at 800 °C for 1 min.

© 2008 Elsevier B.V. All rights reserved.

1. Introduction

Zinc oxide (ZnO) belongs to II–VI compound semiconductor and crystallizes in hexagonal wurtzite structure. At room temperature, ZnO films exhibit very strong emissions by excitons because of the large excitonic binding energy of 60 meV. Furthermore, ZnO has been recognized as a promising photonic material in the UV region due to its wide band gap of 3.37 eV at room temperature [1–7]. So far, various deposition techniques such as sputtering [1,2], molecular beam epitaxy (MBE) [3,4], chemical vapor deposition (CVD) [5,6], and pulsed laser deposition (PLD) [7] have been attempted to grow high-crystalline ZnO films deposited on Si substrates. Among these techniques, the rf magnetron sputtering is the most commonly used technique due to its simple set-up, high deposition rate, and low substrate temperature [1,2].

For depositing high crystal quality ZnO films on Si substrate by rf magnetron sputtering, different deposition conditions such as working pressure, substrate temperature, deposition power, and growth ambient have been considered [1,2]. Unavoidably, the large lattice mismatch and large difference in the thermal expansion coefficients between ZnO films and Si substrates would cause built-in residual stress in the deposited ZnO films [1,8,9]. To improve the crystalline quality of ZnO films grown on Si substrate, the widely known effective technique of thermal annealing treatment can be implemented. There are two kinds of annealing techniques, one is furnace annealing (CFA) and the other is rapid thermal annealing (RTA). Compared to CFA technique, RTA technique offers shorter cycle time, reduced thermal exposure and a lot of size flexibility [10,11]. In view of the advantage of RTA, a study of the controlled details of the RTA parameters for improving the crystal quality of ZnO films should be a subject of great interest. Numerous research works [8,9,12,13] have

* Corresponding author. Tel.: +886 2 86625911; fax: +886 2 26629592.
E-mail address: jacklee@mail.tnu.edu.tw (Y.-C. Lee).

0022-2313/$ - see front matter © 2008 Elsevier B.V. All rights reserved.
doi:10.1016/j.jlumin.2008.09.003

Author's personal copy

indicated an optimum annealing temperature range of 600–900 °C for effective improvement of the crystallinity of ZnO films. However, there are only few reports on the effects of annealing time on the structural and optical properties of ZnO films [14].

In this work, we study the influence of annealing time on the structural and optical properties of ZnO films by the X-ray diffraction (XRD), atomic force microscopy (AFM), and photoluminescence (PL) techniques. The controlled periods of RTA technique for improving the crystal quality of ZnO films will be studied by analyzing the observed XRD patterns and PL spectra.

2. Experiment

Zinc oxide films were deposited by rf magnetron sputtering system using a ZnO target (99.9%). The substrate is p-type silicon with (1 0 0) orientation. Silicon substrates were thoroughly cleaned with organic solvent and dried before loading in the sputtering system. The chamber was pumped down to 1.5×10^{-5} Torr using a diffusion pump before introducing the premixed Ar and O_2 sputtering gases. Throughout all experiments, the target was presputtered for 15 min under 150 W rf power before the onset of the actual deposition in order to remove any contamination on the target surface, enabling the stabilization and optimal operation of the system. In the actual sputtering process, the sputtering power is controlled at 100 W, the sputtering pressure is 1.33 N/m^2, ratio of O_2/Ar is 0.75, distance between substrate and target is 50 mm, and the substrate is not heated. This procedure was adopted to minimize the effect of different positions in the sputtering system and the sputtering time was 1 h. The thickness of as-grown films was examined by α-step to confirm the uniformity and the film thickness was measured to be around 300 nm. Then the as-grown ZnO sample was divided into six small pieces each with the dimension of 1.0 cm × 1.0 cm. Five of the samples were RTA treated under a constant oxygen flow rate of 500 sccm at 800 °C for 0.5, 1, 3, 5 and 10 min, respectively. During the annealing process, the rising or cooling rate of the temperature was kept at 30 °C/s. The XRD patterns of the ZnO films were obtained using Cu Kα radiation ($\lambda=1.5405$ Å). AFM (Veeco Digital Instruments Inc.) measurements with tapping mode and 1 Hz scan rate were made on the ZnO thin films to investigate the surface morphologies. The PL measurements were carried out using the 266 nm line with 5 mW power of a microchip laser (Teem Photonics). The laser beam was focused onto a circular spot of size 1 mm diameter to stimulate luminescence. The luminescence was collected using a spectrometer (Jobin Yvon 550) with a 1200 grooves/mm grating and detected using a cooled GaAs photomultiplier tube.

3. Results and discussion

Fig. 1 displays the XRD patterns of the as-grown and the annealed ZnO films following RTA at 800 °C with different annealing time. All samples exhibiting the prominent (0 0 2) diffraction peak indicate the preferential orientation with the *c*-axis perpendicular to the substrate surface. The (0 0 2) peak position of ZnO films as a function of annealing time is listed in Table 1 and plotted in Fig. 2(a). Since the angular peak position of ZnO powder with (0 0 2) orientation is at $2\theta=34.43^\circ$ [15], the (0 0 2) peak of the as-grown sample shifting to $2\theta=34.36^\circ$ indicates the existence of residual stress between the ZnO film and the Si substrate [1,2,8]. Previous reports showed that the residual stresses in ZnO films contain a thermal stress component and an intrinsic stress component [8,9,16]. The thermal stress is due to the difference in the thermal expansion coefficient (α) between ZnO ($\alpha_{11}=6.05\times10^{-6}\,^\circ\mathrm{C}^{-1}$, $\alpha_{33}=3.53\times10^{-6}\,^\circ\mathrm{C}^{-1}$) and

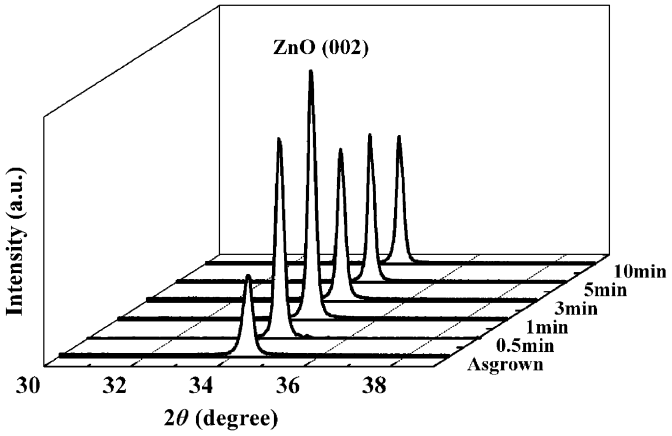

Fig. 1. XRD patterns of the as-grown and the ZnO thin films annealed at 800 °C with different annealing time.

silicon substrate ($\alpha=2.50\times10^{-6}\,^\circ\mathrm{C}^{-1}$) [1]. Because the thermal expansion coefficient of ZnO is bigger than that of silicon substrate, the substrate exerts a resultant tensile stress effect to the ZnO film as the substrate cools down from high temperature to room temperature. On the other hand, intrinsic stress has its origin in the imperfection of the crystallites during growth. Several growth parameters, such as deposition temperature, pressure, power, and gas mixture could contribute to the intrinsic stress. In the literature [8,9,16], it has been shown that intrinsic stress of the as-grown ZnO films is compressive. During the growth process, the magnitude of the compressive stress component is larger than that of the thermal (tensile) stress component, therefore the as-grown ZnO films exhibit an overall compressive residual stress.

As listed in Table 1, the (0 0 2) peak position of the samples annealed for 0.5 and 1 min locates at $2\theta=34.41^\circ$ and 34.44°, respectively. The shift of (0 0 2) peak position toward $2\theta=34.43^\circ$ indicates that the residual stress in the as-grown ZnO film can be effectively reduced by RTA [8,9,12,13]. With increasing the annealing time over 1 min, the (0 0 2) peak position deviates from the powder value but in the opposite direction, indicating a change in the nature of stress [9,15]. The variation of residual stress would influence the lattice constant "*c*" of ZnO films. Table 1 also lists the lattice constant of the as-grown and annealed ZnO films obtained from the (0 0 2) reflection in the X-ray line profile. Compared to the strain-free lattice constant ($c_0=5.206$ Å) [17], the larger value of the lattice constant in the as-grown ZnO film ($c=5.215$ Å) shows that the unit cell is elongated along the *c*-axis and the compressive forces act in the plane of the film [18,19]. By annealing for 0.5 and 1 min, the lattice constant of the annealed ZnO films has decreased to 5.208 and 5.204 Å, respectively. The variation of the lattice constant has clearly shown that the residual stress can be relaxed upon RTA treatment.

The lattice constant can be further utilized to evaluate the average uniform strain, e_{zz} in the lattice along the *c*-axis [18]:

$$e_{zz}=(c-c_0)/c_0 \tag{1}$$

Further, the biaxial film stress σ is related to the measured *c*-axis strain by the relation [12,18]

$$\sigma=[2C_{13}-(C_{11}+C_{12})(C_{33}/C_{13})]e_{zz} \tag{2}$$

where C_{ij} are elastic stiffness constants. For ZnO, we have $C_{13}=106.1$ GPa, $C_{11}=207.0$ GPa, $C_{12}=117.7$ GPa, and $C_{33}=209.5$ GPa [20]. The biaxial stresses for the as-grown and the annealed ZnO films have been derived from Eq. (2) and presented in Table 1 and Fig. 2(b). Obviously, the residual stress of the as-grown ZnO film is compressive. By annealing at 800 °C for 0.5–1 min, the

Author's personal copy

Table 1
The data evaluated from XRD patterns, AFM images, and PL spectra of the ZnO films annealed at 800 °C for a given period of time

Annealing time	XRD					AFM		PL		
	2θ (deg.)	c (Å)	Stress (GPa)	FWHM (deg.)	Grain size (nm)	Roughness (nm)	Grain size (nm)	Peak position (nm)	FWHM (meV)	Intensity ratio $I_{RTA}/I_{as\text{-}grown}$
As-grown	34.36	5.215	−0.775	0.2232	37.3	5.9	120.2	375	157.1	1
0.5 min	34.41	5.208	−0.170	0.1886	44.1	11	197.7	372	98.3	326
1 min	34.44	5.204	0.193	0.1879	44.3	11.3	202.2	372	94.2	412
3 min	34.45	5.202	0.313	0.1833	45.4	11.9	224.6	371	106.6	228
5 min	34.47	5.199	0.554	0.1675	49.7	13.4	301.7	371	110.7	170
10 min	34.48	5.198	0.675	0.1654	50.3	15.2	320.4	370	119.9	86

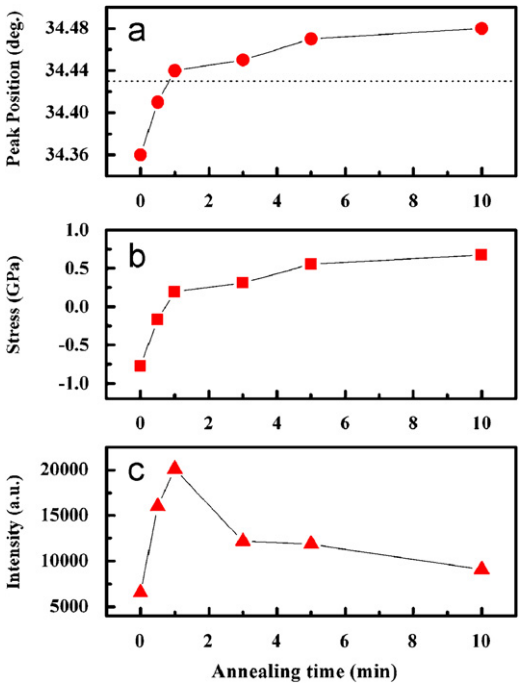

Fig. 2. The (a) peak position, (b) stress, and (c) intensity estimated from the (0 0 2) diffraction peak of XRD for the ZnO films annealed at 800 °C as a function of annealing time.

residual stress of the ZnO films has shown effective relaxation. By further increasing the annealing time, the tensile stress becomes stronger and eventually exceeds the built-in compressive stress and leads to a change in the direction of stress.

Assuming a homogeneous strain across the ZnO films, the average grain size can be estimated from the full-width at half-maximum (FWHM) of (0 0 2) peak by Sherrer's relation [18]

$$D = \frac{0.9\lambda}{B\cos\theta} \tag{3}$$

where λ, θ, and B are the X-ray wavelength, Bragg diffraction angle and FWHM in radians, respectively. From Eq. (3), the grain size for the as-grown sample is 37.3 nm and that for the ZnO film annealed for 0.5 min (1 min) is 44.1 nm (44.3 nm). Previous works have demonstrated that the stress reduction is consistently accompanied by an enhancement in crystallinity, which is manifested by the larger grain size [18,19]. As listed in Table 1, it is noted that when the annealing time increases over 1 min, a decrease in the FWHM of the (0 0 2) peak exhibits an increase in the grain size, while the (0 0 2) peak intensity decreases (shown in Fig. 2(c)). The explanation for the observation of grain size increase together with intensity decrease for annealing time over 1 min may be similar to that of the observation for annealing at higher annealing temperature [18,19], where larger grain growth can result in larger microcracks and rougher surface and lead to lower peak intensity of XRD [19,21]. In addition, Puchert et al. [18] suggested that the annealing-induced optimum improvement in film structure occurs over a reasonably short timescale at higher temperature. From the present experimental observations we conclude that RTA controlled at 800 °C for 0.5–1 min provides the most suitable parameters to improve the crystal quality of ZnO films.

The surface morphology of the as-grown and the annealed ZnO films is studied by AFM images, as shown in Fig. 3 using 2 μm × 2 μm scans. The mean of grain size and the surface roughness are summarized in Table 1. It is noted that the grain size of ZnO films analyzed from AFM is much larger than that from XRD. A probable reason is that the grain size measured from AFM is the surface morphology of coalesced grains which gives the particle size [8]. Nevertheless, the AFM images show that the longer annealing time provides more activation energy to atoms to grow larger grains, which is consistent with the results of XRD. In Fig. 3, it is also observed that the grain boundaries were fewer and the grains grew much bigger with further increase of annealing time. Lin et al. [22] described that high temperature can stimulate the migration of grain boundaries and cause the coalescence of more grains during the annealing processes. Fang et al. [8] further indicated at high temperature, more energy should be available for the atoms to acquire so that they may diffuse and occupy the correct site in the crystal lattice and grains with lower surface energy will grow larger at high temperature. The major grain growth also yields an increase in the surface roughness as shown by previous studies [9,14].

The relationship between the crystallinity and the optical properties of ZnO films annealed with different periods is investigated by PL technique. Fig. 4 shows the 12 K PL spectra in the wavelength range of 330–600 nm for the ZnO films following RTA as a function of annealing time. It is noted that the PL spectra have been normalized with respect to the peak amplitude to facilitate comparison. As shown in Fig. 4(a), the PL spectrum of the as-grown sample exhibits a strong peak at about 375 nm (3.30 eV) with a weak and broad deep-level (DL) emission in the visible range between 450 and 550 nm. The strong PL signal has been assigned to be the UV near-band-edge (NBE) transition, which is directly related to the crystal quality of ZnO [3–5]. On the other hand, the weak signal is commonly regarded as the defect level of oxygen vacancies because the generation of oxygen vacancies during deposition is unavoidable for the as-grown ZnO films. It is well known that the relations between the luminescence properties and crystal quality of ZnO films can be discussed by the intensity ratio of the NBE emission to the DL emission in the PL spectra. However, in our work, the weak DL emission has been only observed in the as-grown ZnO film. The reason for this result is that the films grown under oxygen-rich ambient have absorbed more oxygen atoms during the growth process and the

Author's personal copy

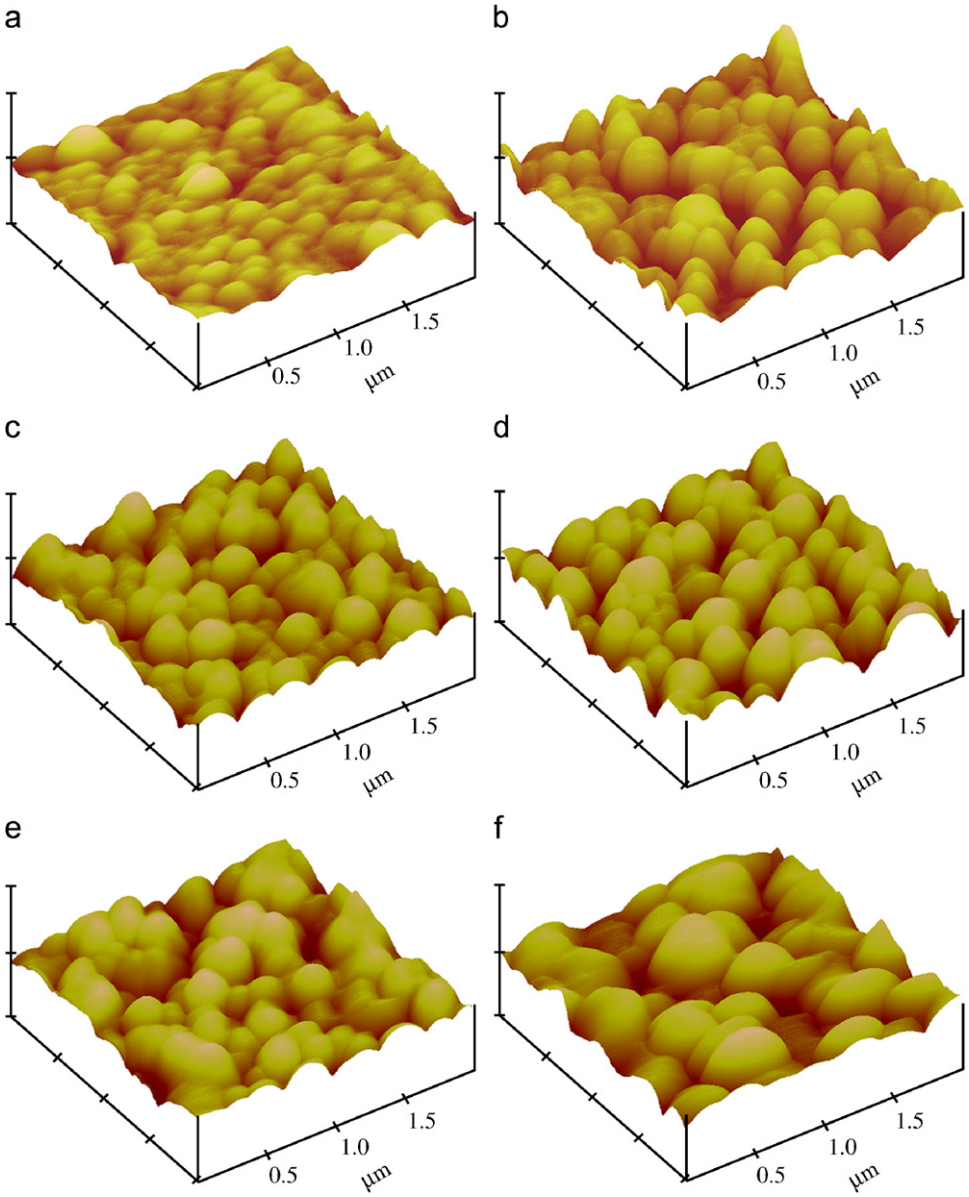

Fig. 3. AFM images of ZnO thin films: (a) as-grown and RTA at 800 °C for (b) 0.5 min, (c) 1 min, (d) 3 min, (e) 5 min, and (f) 10 min.

as-deposited films have only few oxygen vacancies [23,24]. Furthermore, no obvious DL emission can be detected for the treated samples regardless of the annealing time, indicating an effective reduction of oxygen vacancies after RTA in oxygen-rich ambient. In the literature by Shan et al. [24], they concluded that oxygen would diffuse into the lattice to fill the oxygen vacancies during annealing process; therefore the annealing process in oxygen can enhance the NBE emission and quenched the DL emission.

The as-measured PL spectra in the UV region are redisplayed in Fig. 5. It is clearly observed that both the position (band gap energy) and intensity of the PL peak can be affected by RTA. The peak position, the fitted FWHM and the intensity ratio ($I_{RTA}/I_{as\text{-}grown}$) of the NBE of PL signal as a function of annealing period are listed in Table 1. The PL spectra in Fig. 5 exhibits the UV peak position (band-gap energy) shifted from 375 nm (3.30 eV) to 370 nm (3.35 eV) with increasing annealing time. The blue shift of band-gap energy has been attributed to originate from the residual stress along the *c*-axis of ZnO due to lattice distortion [12]. As illustrated from the analysis of XRD spectra, the lattice constant showed decrease following RTA treatments, and thus resulting in the stress being changed from compressive to tensile, as manifested by the blue shift of the band gap energy. Moreover, at 12 K, the FWHM of PL signal of the as-grown ZnO film is about 157.1 meV and that of the ZnO film annealed for 1 min can be effectively reduced to be about 94.2 meV. A narrower PL linewidth and higher PL intensity are regarded as a clear evidence for the improvement of crystal quality [12,15]. However, by increasing the annealing time over 1 min, the FWHM and intensity of PL of the annealed ZnO films become broader and lower, respectively. It indicates that the crystallinity of ZnO film annealed for a prolonged period becomes unsuitable for optical application. A plausible reason is that the decrease in the length of *c*-axis of ZnO films annealed for a prolonged period may induce an acute lattice distortion, which would significantly affect the optical properties of ZnO films and quench the PL efficiency [12,15]. The other reason as suggested by Zu et al. [25] is that an average grain size of ~55 nm exhibited weaker luminescence emission because grain size much larger than the exciton Bohr radius in ZnO would decrease the quantum efficiency of luminescence. As plotted in

Author's personal copy

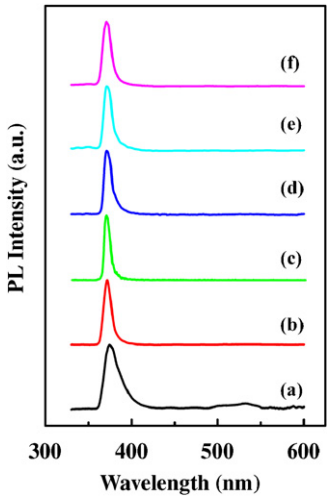

Fig. 4. The 12 K PL spectra of the as-grown and RTA-treated ZnO thin films: (a) as-grown and RTA at 800 °C for (b) 0.5 min, (c) 1 min, (d) 3 min, (e) 5 min, and (f) 10 min.

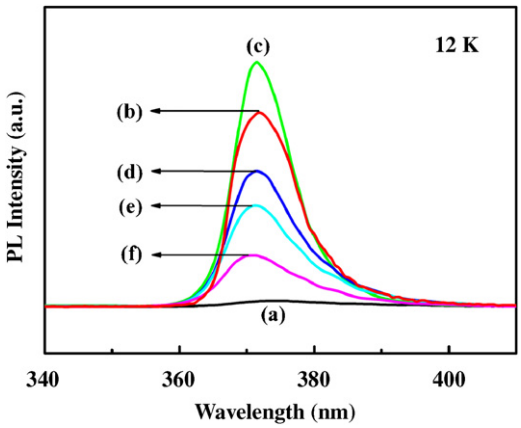

Fig. 5. Band-edge PL spectra at 12 K of the as-grown and RTA-treated ZnO thin films: (a) as-grown and RTA at 800 °C for (b) 0.5 min, (c) 1 min, (d) 3 min, (e) 5 min, and (f) 10 min.

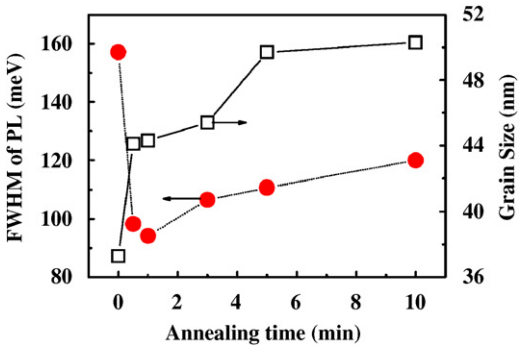

Fig. 6. The fitted FWHM of PL at 12 K and the grain sizes estimated from XRD patterns for the ZnO films annealed at 800 °C as a function of annealing time.

Fig. 6, the ZnO film annealed with increasing annealing time leads to a grain size close to 55 nm, and exhibits a degradation of PL signals. In addition, the variations of *c*-axis length and grain size between the samples annealed for 5 and 10 min are not obvious, but the PL intensity of ZnO annealed for 10 min is only half that of ZnO annealed for 5 min. According to the AFM images, the surface of ZnO film annealed for 10 min becomes much rougher and exhibits much larger height variation than that of ZnO film annealed for 5 min. Liu et al. [14] suggested that the structural changes would increase the volume fraction of the "voids" on the surface of ZnO film and the increase in the volume fraction of the "voids" would reduce the optical properties, which may explain the difference between the PL intensity of ZnO film annealed for 5 and 10 min.

4. Conclusion

In summary, we have discussed the effects of annealing time on the structural and optical properties of sputtered ZnO films. Following RTA treatment, the annealed ZnO films show stronger intensity and narrower FWHM of the (0 0 2) XRD peak. Compared to the as-grown ZnO film, the residual compressive stress can be relaxed via RTA treatment to improve the crystal quality of the ZnO film. Further, the ZnO film annealed at 800 °C for 1 min shows the best PL efficiency. We have demonstrated that RTA treatment can be an effective and efficient technique to release built-in stress, which leads to an enhancement of crystallinity and more efficient UV luminescence properties of ZnO film.

Acknowledgements

The author Y.C. Lee would like to acknowledge the support of the National Science Council Project no. NSC 96-2112-M-236-001-MY3. S.Y. Hu acknowledges the support of the National Science Council Project no. NSC 95-2745-M-272-001.

References

[1] W. Water, S.Y. Chu, Mater. Lett. 55 (2002) 67.
[2] T. Shimomura, D. Kim, M. Nakayama, J. Lumin. 112 (2005) 191.
[3] M.J.H. Henseler, W.C.T. Lee, P. Miller, S.M. Durbin, R.J. Reeves, J. Cryst. Growth 287 (2006) 48.
[4] S.H. Jeong, B.S. Kim, B.T. Lee, Appl. Phys. Lett. 82 (2003) 2625.
[5] K. Haga, T. Suzuki, Y. Kashiwaba, H. Watanabe, B.P. Zhang, Y. Segawa, Thin Solid Films 433 (2003) 131.
[6] J.D. Ye, S.L. Gu, S.M. Zhu, F. Qin, S.M. Liu, W. Liu, X. Zhou, L.Q. Hu, R. Zhang, Y. Shi, Y.D. Zheng, J. Appl. Phys. 96 (2004) 5308.
[7] H.S. Kang, J.S. Kang, S.S. Pang, E.S. Shim, S.Y. Lee, Mater. Sci. Eng. B 102 (2003) 313.
[8] Z.B. Fang, Z.J. Yan, Y.S. Tan, X.Q. Liu, Y.Y. Wang, Appl. Surf. Sci. 241 (2005) 303.
[9] M. Wang, J. Wang, W. Chen, Y. Cui, L. Wang, Mater. Chem. Phys. 97 (2006) 219.
[10] T.Y. Ma, D.K. Shim, Thin Sold Films 410 (2002) 410.
[11] K.K. Kim, S. Niki, J.Y. Oh, J.O. Song, T.Y. Seong, S.J. Park, S. Fujita, S.W. Kim, J. Appl. Phys. 97 (2005) 066103.
[12] R. Hong, J. Huang, H. He, Z. Fan, J. Shao, Appl. Surf. Sci. 242 (2005) 346.
[13] M.L. Cui, X.M. Wu, L.J. Zhuge, Y.D. Meng, Vacuum 81 (2007) 899.
[14] Y.C. Liu, S.K. Tung, J.H. Hsieh, J. Cryst. Growth 287 (2006) 105.
[15] P. Sagar, P.K. Shishodia, R.M. Mehra, H. Okada, A. Wakahara, A. Yoshida, J. Lumin. 126 (2007) 800.
[16] A. Cimpoiasu, N.M. van der Pers, Th.H. de Keyser, A. Venema, M.J. Vellekoop, Smart Mater. Struct. 5 (1996) 744.
[17] R.D. Vispute, V. Talyansky, S. Choopun, R.P. Sharma, T. Venkatesan, M. He, X. Tang, J.B. Halpern, M.G. Spencer, Y.X. Li, L.G. Salamanca-Riba, A.A. Iliadis, K.A. Jones, Appl. Phys. Lett. 73 (1998) 348.
[18] M.K. Puchert, P.Y. Timbrell, R.N. Lamb, J. Vac. Sci. Technol. A 14 (1996) 2220.
[19] V. Gupta, A. Mansingh, J. Appl. Phys. 80 (1996) 1063.
[20] D. Singh, Y.P. Varshni, Phys. Rev. B 24 (1981) 4340.
[21] Z. Fang, Y. Wang, D. Xu, Y. Tan, X. Liu, Opt. Mater. 26 (2004) 239.
[22] Y. Lin, J. Xie, H. Wang, Y. Li, C. Chavez, S. Lee, S.R. Foltyn, S.A. Crooker, A.K. Burrell, T.M. McCleskey, Q.X. Jia, Thin Solid Films 101 (2005) 492.
[23] Z.Y. Wang, L.Z. Hu, J. Zhao, J. Sun, Z.J. Wang, Vacuum 78 (2005) 53.
[24] F.K. Shan, G.X. Liu, W.J. Lee, B.C. Shin, J. Appl. Phys. 101 (2007) 053106.
[25] P. Zu, Z.K. Tang, G.K.L. Wong, M. Kawasaki, A. Ohtomo, H. Koinuma, Y. Segawa, Solid State Commun. 103 (1997) 459.